Turkish **J**ournal of **M**athematics and **C**omputer **S**cience
TJMCS

http://tjmcs.matder.org.tr/

A numerical solution of the equal width wave equation using a fully implicit finite difference method

Bilge İNAN and Ahmet Refik BAHADIR

Abstract.
In this paper, a fully implicit finite difference scheme for the numerical solution of the equal width wave (EW) equation is proposed. Since the EW equation is nonlinear the scheme leads to a system of nonlinear equations. At each time-step Newton's method is used to solve this nonlinear system. The results and comparisons with analytical and other numerical values clearly show that results obtained using the fully implicit finite difference scheme are precise and reliable.

2010 AMS Classification: 65M06, 74J35
Keywords: Equal width wave equation; Finite differences; Solitary waves; Undular bore; Nonlinear partial differential equations

1. Introduction

The non-linear equal width wave (EW) equation, derived for long waves propagating with dispersion processes, has the following form,

$$\frac{\partial u}{\partial t} + u\frac{\partial u}{\partial x} - \mu\frac{\partial}{\partial t}\left(\frac{\partial^2 u}{\partial x^2}\right) = 0 \tag{1.1}$$

where u is the wave amplitude, μ is a positive parameter. The equation was introduced by Morrison et al. [12].

The analytical solutions of the EW equation are only possible for certain conditions. Therefore numerical solution techniques are usually needed. Several numerical methods have been used for this purpose. Gardner *et al.* [8] solved the EW equation using Galerkin method with cubic B-spline finite elements. Archilla [2] developed a numerical method using a spectral Fourier discretization for the spatial derivatives. Gardner *et al.* [9] investigated Petrov-Galerkin method with quadratic B-spline finite elements for the solution of the equation. Khalifa *et al.* [11] employed a finite element method using quintic splines as element shape function for the EW equation. Zaki [18, 19] solved the equation by a least-squares technique using linear space-time finite elements and Petrov-Galerkin finite element scheme with shape functions taken as quadratic B-spline functions, respectively. An approach based on a collocation method incorporated cubic B-splines was proposed by Dag and Saka [4]. Raslan [14] proposed a collocation method based on quintic B-spline

finite elements to solve the EW equation. Esen [6] applied a lumped Galerkin method based on quadratic B-spline finite elements for solving the equation. Dogan [5] described Galerkin's method using linear finite elements to the equal width wave equation. Using the fourth-order Runge-Kutta method a numerical simulation and explicit solution of the EW equation were obtained by Raslan [15]. A solution based on a quadratic B-spline finite element and splitting technique is investigated by Saka [16]. A linearized implicit finite difference method is applied to this equation by Esen and Kutluay [7]. Ramos [13] described some explicit finite difference methods to obtained numerical solutions to the EW and RLW equations. Recently, Saka et al. [17] solved the equation using a Galerkin method based on quartic B-spline finite elements, a differential quadrature method with cosine expansion basis and collocation method with radial-basis unctions. Ali [1] used the spectral method based on Chebyshev polynomials for solving the equal width wave equation. The reduced differential transform method was applied to find the numerical solution of the equation by Arora *et al*. [3]. Numerical solutions of the equal width wave equation was obtained by Septic B-Spline collocation method using Rubin and Graves linearization technique[10].

In the present work, a fully implicit finite difference scheme is applied to obtain the solution of the EW equation. Some examples are presented to show the ability of the method. Solutions obtained from this method are compared with the previous results reported in the literature.

2. The Method of Solution

The discretization was done by the finite differences with the implicit approach. Solution domain is discretized into cells described by the nodes set (x_i, t_n) in which $x_i = ih$, $(i = 0, 1, 2, \ldots, N)$ and $t_n = nk$, $(n = 0, 1, 2, \ldots)$, h is the spatial mesh size and k is the time step.

A fully implicit discretization for Eq.(1.1) takes the following form

$$\frac{U_i^{n+1} - U_i^n}{k} + \frac{1}{4}\left[\frac{\left(U_{i+1}^{n+1}\right)^2 - \left(U_{i-1}^{n+1}\right)^2}{2h} + \frac{\left(U_{i+1}^{n}\right)^2 - \left(U_{i-1}^{n}\right)^2}{2h}\right]$$

$$- \frac{\mu}{k}\left[\frac{U_{i+1}^{n+1} - 2U_i^{n+1} + U_{i-1}^{n+1}}{h^2} - \frac{U_{i+1}^{n} - 2U_i^{n} + U_{i-1}^{n}}{h^2}\right] = 0 \tag{2.1}$$

which is valid for values of i lying in the interval $1 \le i \le N-1$. Where U_i^n denotes the finite difference approximation to the exact solution $u(x,t)$. Eq.(2.1) is a system of nonlinear difference equation. Let us consider this nonlinear system of equations in the form

$$F(V) = \mathbf{0} \tag{2.2}$$

where $F = [f_1, f_2, \ldots, f_{N-1}]^T$ and $V = \left[U_1^{n+1}, U_2^{n+1}, \ldots, U_{N-1}^{n+1}\right]^T$. Newton's method applied to Eq.(2.2) results in the following iteration:

1. Set $V^{(0)}$, an initial guess.
2. For $m = 0, 1, 2, \ldots$ until convergence do:
   Solve $J(V^{(m)})\delta^{(m)} = -F(V^{(m)})$;

Set $V^{(m+1)} = V^{(m)} + \delta^{(m)}$

where $J(V^{(m)})$ is the Jacobian matrix which is evaluated analytically. The solution at the previous time-step is taken as the initial estimate. The convergence is generally obtained in two or three iterations.

3. Test Problems and Discussion

In this section, some test problems have been considered to illustrate the performance of the method described in previous section. The accuracy of the method is measured by using the L_2 and L_∞ norms defined by

$$\begin{aligned} L_2 &= \|u-U\|_2 = \left(h\sum_{i=0}^{N}|u_i-U_i|^2\right)^{\frac{1}{2}}, \\ L_\infty &= \|u-U\|_\infty = \max_{0\le i\le N}|u_i-U_i| \end{aligned} \tag{3.1}$$

where u and U represent the exact and approximate solutions, respectively.

We also examined our results by calculating the following three conserved quantities corresponding to mass, momentum and energy, respectively[9].

$$I_1 = \int_{-\infty}^{+\infty} u dx$$

$$I_2 = \int_{-\infty}^{+\infty} \left(u^2 + \mu\,(u_x)^2\right) dx \tag{3.2}$$

$$I_3 = \int_{-\infty}^{+\infty} u^3 dx$$

Motion of single solitary wave

We first model the motion of a single solitary wave of the EW equation. The solitary wave solution of the EW equation (1.1) is

$$u(x,t) = 3c\,\mathrm{sec}\,h^2(q(x-x^*-ct)) \tag{3.3}$$

with amplitude $3c$ where c is the wave velocity and $q = (1/4\mu)^{1/2}$ measures width of the wave pulse. The initial and boundary conditions are set to: $u(x,0) = 3c\,\mathrm{sec}\,h^2(q(x-x^*))$ and $u \longrightarrow 0$ as $x \longrightarrow \pm\infty$, respectively.

The analytical values of conservation quantities can be found as

$$I_1 = \frac{6c}{q}, \qquad I_2 = \frac{12c^2}{q} + \frac{48qc^2\mu}{5} \quad \text{and} \quad I_3 = \frac{144c^3}{5q}. \tag{3.4}$$

To allow comparison with the previous methods parameters are taken as $x^* = 10$ and $\mu = 1$ through the interval $0 \le x \le 30$.

The analytical invariants obtained from Eq. (3.4) are $I_1 = 1.20000$, $I_2 = 0.28800$ and $I_3 = 0.05760$ for $c = 0.1$. Table 1 displays the invariants and error norms for $c = 0.1$, $h = 0.03$ and $k = 0.05$ through the interval $0 \le x \le 30$. The invariants and error norms of the proposed scheme are given for times up to $t = 80$ in Table 1. In Table 1, the L_2 error norm reaches a maximum of 1.2476×10^{-4} at the end of the run. A comparison of the invariants and error norms obtained by the present method and the result of references [4, 5, 6, 9, 16] are given in Table 2 for $c = 0.1$, $h = 0.03$ and $k = 0.05$ at $t = 80$.

Table 1
Invariants and error norms for the single solitary wave.

t	I_1	I_2	I_3	$L_2 \times 10^3$	$L_\infty \times 10^3$
0	1.19994	0.28800	0.05760		
10	1.20001	0.28800	0.05760	0.03296	0.03342
20	1.20004	0.28800	0.05760	0.05474	0.04571
30	1.20005	0.28800	0.05760	0.07214	0.05023
40	1.20005	0.28800	0.05760	0.08651	0.05255
50	1.20005	0.28800	0.05760	0.09835	0.05871
60	1.20005	0.28800	0.05760	0.10824	0.06376
70	1.20005	0.28800	0.05760	0.11685	0.06827
80	1.20004	0.28800	0.05760	0.12476	0.07254

Table 2
Comparison of invariants for the single solitary wave.

	I_1	I_2	I_3
Present Method	1.20004	0.28800	0.05760
[4]	1.19998	0.28798	0.05759
[5]	1.23387	0.29915	0.06097
[6]	1.19995	0.28798	0.05759
[9]	1.1910	0.2855	0.05582
[16]	1.19999	0.28801	0.05760

The analytical value of invariants are $I_1 = 0.36000$, $I_2 = 0.02592$ and $I_3 = 0.00156$ for $c = 0.03$. The invariants and error norms are displayed in Table 3 for $c = 0.03$, $h = 0.05$ and $k = 0.05$ through a region $0 \le x \le 30$. In Table 3, the L_2 error norm reaches a maximum of 4.360×10^{-5} at $t = 80$. Comparison of the invariants and error norms are found by the present method and by the other methods [5, 6, 16] are given in Table 4 for $c = 0.03$, $h = 0.05$ and $k = 0.05$ at $t = 80$.

Table 3
Invariants and error norms for the single solitary wave.

t	I_1	I_2	I_3	$L_2 \times 10^3$	$L_\infty \times 10^3$
0	0.35998	0.02592	0.00156		
10	0.35999	0.02592	0.00156	0.00634	0.00403
20	0.36000	0.02592	0.00156	0.01233	0.00810
30	0.36000	0.02592	0.00156	0.01806	0.01231
40	0.36001	0.02592	0.00156	0.02356	0.01648
50	0.36001	0.02592	0.00156	0.02888	0.02051
60	0.36001	0.02592	0.00156	0.03399	0.02430
70	0.36001	0.02592	0.00156	0.03890	0.02778
80	0.36001	0.02592	0.00156	0.04360	0.03095

Table 4
Comparison of the invariants for the single solitary wave.

	I_1	I_2	I_3
Present Method	0.36001	0.02592	0.00156
[5]	0.36665	0.02658	0.00162
[6]	0.36000	0.02592	0.00156
[16]	0.36000	0.02592	0.00156

The analytical values of invariants are in good agreements the numerical values of invariants are given in both Table 1 and Table 3. The numerical solution for $c = 0.1$ and $c = 0.03$ is shown in Fig. 1 and Fig. 2, respectively. It can be seen from Fig. 1a and Fig. 2a, the single solitary wave moves to the right at constant speed with unchanged amplitude both $c = 0.1$ and $c = 0.03$. The figures present the wave velocity increases when the value of the amplitude increases.

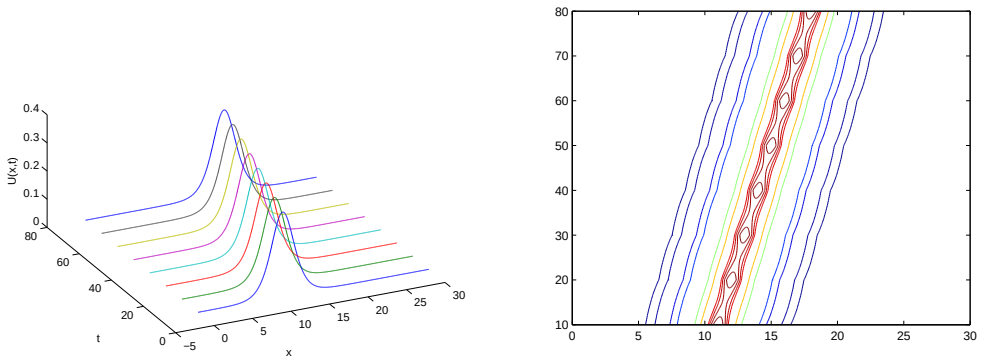

FIGURE 1. Numerical solutions of the single solitary wave with $c = 0.1$.

We displayed the countours of the tests for $c = 0.1$ and $c = 0.03$ in Fig. 1b and Fig. 2b, respectively. The agreement between numerical and analytical solution is good for this

problem. Furthermore, It is observed that the values of I_1, I_2 and I_3 remain almost constant during the computer run.

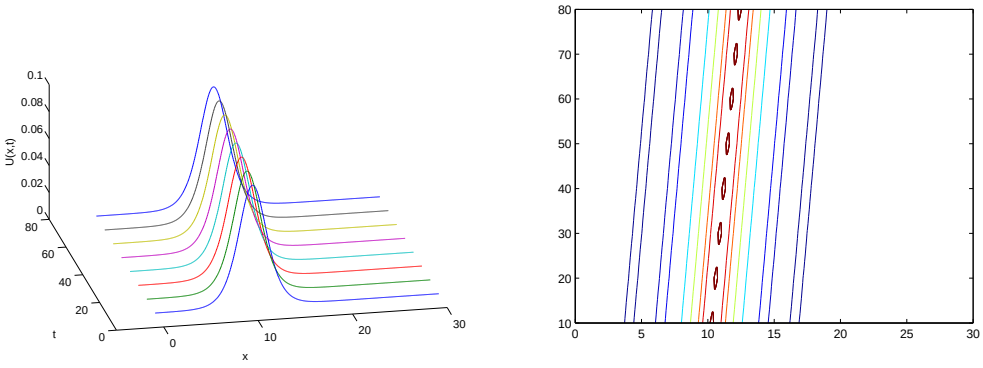

(a) (b)

FIGURE 2. Numerical solutions of the single solitary wave with $c = 0.03$.

Interaction of two solitary waves

Secondly, the interaction process of two solitary waves traveling in the same direction is studied by using the initial condition

$$u(x,0) = 3c_1 \sec h^2(q_1(x - x_1^* - c_1)) + 3c_2 \sec h^2(q_2(x - x_2^* - c_2)) \tag{3.5}$$

and the boundary condition $u \longrightarrow 0$ as $x \longrightarrow \pm\infty$.

In this case, to make comparison with other works we take the following parameters: $c_1 = 1.5$, $c_2 = 0.75$, $q_1 = 0.5$, $q_2 = 0.5$, $h = 0.1$, $k = 0.1$, $x_1^* = 10$, $x_2^* = 25$ and $\mu = 1$ over the region $0 \le x \le 80$.

The analytical values of the invariants quantities are

$$I_1 = 12(c_1 + c_2),\ I_2 = 28.8(c_1^2 + c_2^2) \text{ and } I_3 = 57.6(c_1^3 + c_2^3). \tag{3.6}$$

Thus $I_1 = 27$, $I_2 = 81$ and $I_3 = 218.7$ are found from Eq. (3.6).

In Table 5, the numerical values of the invariants are displayed for interaction of the two solitary waves. The numerical values of the invariants are given in Table 5 are in good agreements the analytical values of them.

Table 5
Invariants for the interaction of two solitary waves.

t	I_1	I_2	I_3
1	27.00009	81.00024	218.70236
5	27.00018	80.99985	218.69987
10	27.00018	80.99500	218.65881
15	27.00018	80.95157	218.32090
20	27.00018	80.99355	218.64833
25	27.00018	80.99903	218.69551
30	27.00018	80.99883	218.69574

Table 6
Comparison of invariants for the interaction of two solitary waves at $t = 30$.

	Present Method	[6]	[7]	[17]
I_1	27.00018	27.00003	27.00017	27.00017
I_2	80.99883	81.01719	80.96848	81.00044
I_3	218.69574	218.70650	218.70210	218.70304

We displayed the interaction of two solitary waves from $t = 0$ to $t = 30$ in Fig. 3. The larger wave catches up with the smaller wave while time increases. It can also clearly be seen from the countours of the results in Fig. 4. A comparison of the numerical values of the invariants obtained by the present method and by other methods [6, 7, 17] are displayed in Table 6.

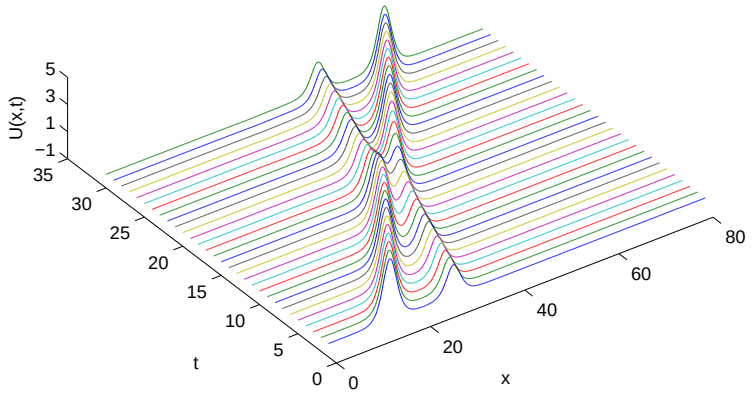

FIGURE 3. The interaction of two solitary waves.

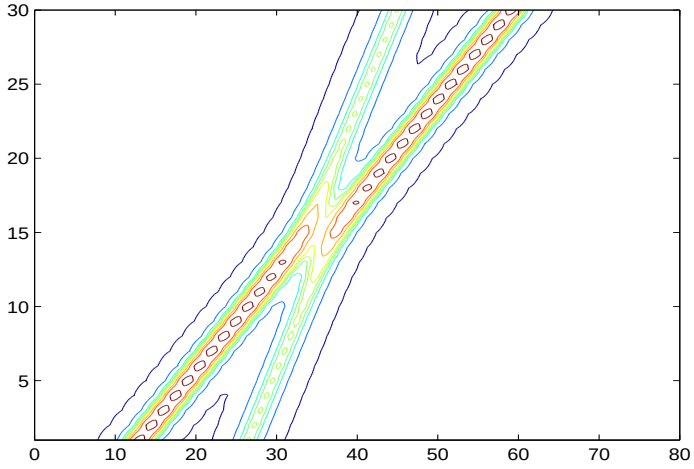

FIGURE 4. The countours of interaction of two solitary waves.

The undular bore

To model the development of an undular bore we use the initial condition given by

$$u(x,0) = \frac{u_0}{2}(1 - \tanh(\frac{x - x^*}{d})) \tag{3.7}$$

with the boundary condition $u(a,t) = u_0$ and $u(b,t) = 0$. In that case, variations in three invariants are as follows

$$\begin{aligned} M_1 &= \frac{dI_1}{dt} = \frac{1}{2}u_0^2, \\ M_2 &= \frac{dI_2}{dt} = \frac{2}{3}u_0^3, \\ M_3 &= \frac{dI_3}{dt} = \frac{3}{4}u_0^4. \end{aligned} \tag{3.8}$$

As seen from the values they are increased linearly at a rate of M_j, $(j = 1,2,3)$ [9]. Thus theorical variations in the invariants $M_1 = 5 \times 10^{-3}$, $M_2 = 6.66667 \times 10^{-4}$ and $M_3 = 7.5 \times 10^{-5}$ obtained from Eq. (3.8).

In this problem, following parameters are taken: $\mu = 0.1666667$, $u_0 = 0.1$ and $x^* = 0$ through the interval $-20 \le x \le 50$. Numerically variations in invariants can be computed from following equation [17].

$$M_j = \frac{I_j(\text{at } t = 800) - I_j(\text{at } t = 0)}{\text{time}}, \ j = 1,2,3 \tag{3.9}$$

Table 7 presents I_1, I_2 and I_3, the position and amplitude for the gentle slope $d = 5$. The variations of the invariants obtained from the present method compared with the variations of invariants are given in [4, 6, 16] are shown in Table 8.

Table 7
Invariants for the undular bore with $h = 0.07$, $k = 0.5$ and $d = 5$.

t	I_1	I_2	I_3	x	U
0	1.996585	0.174778	0.016218		
200	2.996424	0.308051	0.031215	8.77	0.160497
400	3.996422	0.441289	0.046224	20.39	0.179242
600	4.996422	0.574524	0.061233	32.50	0.182617
800	5.996420	0.707759	0.076242	44.75	0.183677
800[4]$(h = k = 0.05)$	6.003096	0.708689	0.076281	44.75	0.18397
800[6]$(h = 0.07, k = 0.05)$	6.003578	0.708498	0.076192	44.75	0.183822
800[16]$(h = k = 0.05)$	6.00259	0.70885	0.07628	44.75	0.184050

Table 8
Comparison of the variations in invariants for the undular bore with $h = 0.07$, $k = 0.5$ and $d = 5$.

	$M_1 \times 10^3$	$M_2 \times 10^4$	$M_3 \times 10^5$
Present Method	4.99979	6.66226	7.50300
[4]$(h = k = 0.05)$	5.00065	6.66639	7.5005
[6]$(h = 0.07, k = 0.05)$	5	6.66275	7.4875
[16]$(h = k = 0.05)$	5	6.668375	7.5

The values of I_1, I_2 and I_3, the position and amplitude are shown in Table 9 for $d = 2$. Table 10 displays comparison of the variations in the invariants obtained by the present method together with the other methods [4, 6, 16].

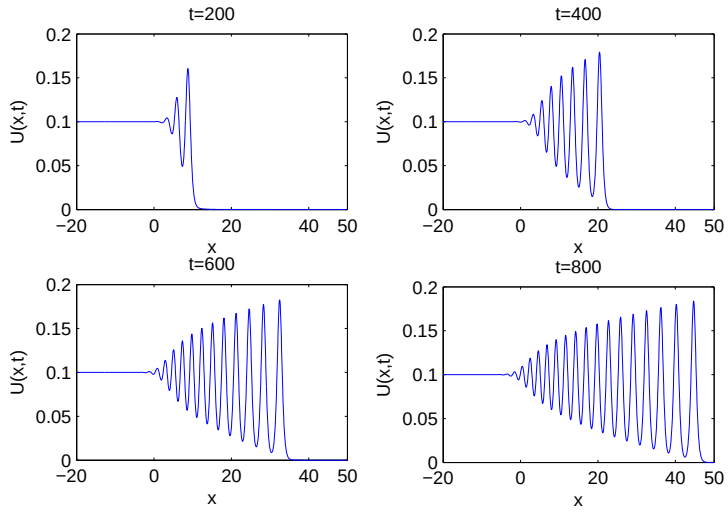

FIGURE 5. Undular bore for $d = 5$ at different times.

Table 9
Invariants for the undular bore with $h = 0.07$, $k = 0.5$ and $d = 2$.

t	I_1	I_2	I_3	x	U
0	1.996500	0.189928	0.018465		
200	2.996500	0.323191	0.033471	9.40	0.175870
400	3.996500	0.456426	0.048480	21.37	0.181976
600	4.996500	0.589660	0.063489	33.55	0.183831
800	5.996477	0.722894	0.078498	45.87	0.184426
800[4]($h = k = 0.05$)	6.003194	0.723867	0.078534	45.85	0.18460
800[6]($h = 0.07, k = 0.05$)	6.003478	0.723605	0.078426	45.87	0.184518
800[16]($h = k = 0.05$)	6.00248	0.72402	0.07853	45.85	0.184713

Table 10
Comparison of the variations in invariants for the undular bore with $h = 0.07$, $k = 0.5$ and $d = 2$.

	$M_1 \times 10^3$	$M_2 \times 10^4$	$M_3 \times 10^5$
Present Method	4.99997	6.66208	7.50413
[4]($h = k = 0.05$)	5.00087	6.66674	7.5011
[6]($h = 0.07, k = 0.05$)	5	6.662	7.4862
[16]($h = k = 0.05$)	5	6.668625	7.5

Fig. 5 displays the undular bore profiles for the gentle slope $d = 5$ from $t = 200$ to $t = 800$ for each 200 time steps. It is seen from Fig. 5, the number of waves increases with increase of t. As can be seen from Fig. 6, value of d decreased with the number of waves increase, as expected.

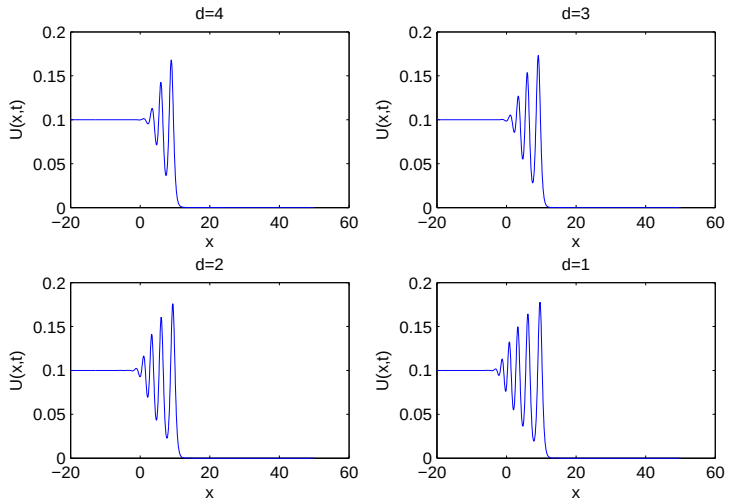

FIGURE 6. Undular bore for different values of d at $t = 200$.

The Maxwellian initial condition

Finally, we use the initial condition

$$u(x, 0) = \exp(-(x - 7)^2) \tag{3.10}$$

and the boundary condition $u \longrightarrow 0$ as $x \longrightarrow \pm\infty$ to analyse the evolution of an Maxwellian pulse into solitary waves.

In this test, we study for values of $\mu = 0.2$, $\mu = 0.04$ and $\mu = 0.001$ through the interval $0 \leq x \leq 12$.

Table 11 gives a comparison of the invariants obtained from the present method for $h = k = 0.01$ and the invariants are obtained in [1, 15].

i) The variations of I_1, I_2, I_3 are obtained from Table 11 for $\mu = 0.2$ as 1.690214×10^{-4}, 2.6572×10^{-6} , 2.375×10^{-7}whereas they obtained as 2.2×10^{-3}, 6.3×10^{-2} , 3×10^{-6} in [1] and 2.387×10^{-2}, 8×10^{-2} , 1.8×10^{-5} in [15], respectively.

ii) The variations of I_1, I_2, I_3 for $\mu = 0.04$ are found as 1.63×10^{-8}, 3.14405×10^{-5}, 7.0149×10^{-6} also they obtained as 2.2×10^{-3}, 7.5×10^{-2}, 3×10^{-6} in [1] and 7×10^{-3}, 2.248×10^{-3}, 9.6×10^{-5} in [15], respectively.

iii) For $\mu = 0.001$, the change of I_1, I_2, I_3 are obtained from Table 11 as 6×10^{-15}, 1.5655707×10^{-3}, 6.842706×10^{-4} whereas they obtained as 1.2×10^{-2}, 7.8×10^{-2}, 3×10^{-6} in [1] and 1.16×10^{-2}, 6.42×10^{-4}, 1.9×10^{-5} in [15], respectively.

Fig. 7 shows wave profiles for the Maxwellian initial condition at $t = 25$ and for $0 \leq x \leq 60$. This figure contains figures for $\mu = 0.2$, $\mu = 0.04$ and $\mu = 0.001$, respectively. As can be seen from Fig. 7, μ is reduced, more and more solitary waves are formed, as expected.

Table 11
Invariants for Maxwellian initial condition.

		Present Method			[1]			[15]		
μ	t	I_1	I_2	I_3	I_1	I_2	I_3	I_1	I_2	I_3
0.2	0.5	1.772444	1.503977	1.023327	1.772454	1.503977	1.023327	1.772454	1.503339	1.023327
	1.0	1.772432	1.503977	1.023327	1.773063	1.508032	1.023328	1.772457	1.503303	1.023327
	2.0	1.772400	1.503976	1.023327	1.773604	1.520078	1.023329	1.772531	1.503190	1.023328
	3.0	1.772353	1.503975	1.023327	1.774116	1.539771	1.023329	1.774443	1.505232	1.023329
	4.0	1.772285	1.503974	1.023326	1.774653	1.566542	1.023330	1.796324	1.583276	1.023345
0.04	0.5	1.772454	1.303446	1.023327	1.772454	1.303447	1.023327	1.772454	1.303289	1.023328
	1.0	1.772454	1.303445	1.023326	1.773063	1.308312	1.023328	1.772453	1.303178	1.023331
	2.0	1.772454	1.303440	1.023325	1.773603	1.322768	1.023329	1.772454	1.302571	1.023355
	3.0	1.772454	1.303430	1.023323	1.774114	1.346399	1.023329	1.772447	1.301551	1.023400
	4.0	1.772454	1.303415	1.023320	1.774648	1.378525	1.023330	1.765447	1.301041	1.023424
0.001	0.5	1.772454	1.254566	1.023326	1.772453	1.254567	1.023327	1.772453	1.254567	1.023326
	1.0	1.772454	1.254563	1.023324	1.772454	1.259631	1.023328	1.772454	1.254566	1.023327
	2.0	1.772454	1.254532	1.023310	1.772453	1.274673	1.023329	1.772453	1.254304	1.023330
	3.0	1.772454	1.254209	1.023161	1.772434	1.299265	1.023329	1.772434	1.253925	1.023327
	4.0	1.772454	1.253002	1.022642	1.760800	1.332696	1.023330	1.760800	1.255103	1.023311

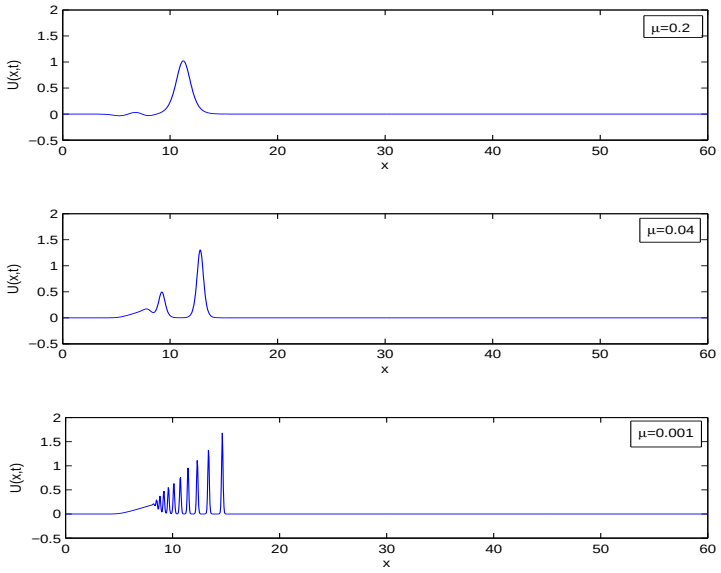

FIGURE 7. Maxwellian initial condition for different values of μ at $t = 25$.

4. CONCLUSION

In this paper a fully implicit finite difference method was applied to the EW equation. Numerical tests for single solitary wave and interaction of two solitary waves are given. We also have examined two development of an undular bore and evolution of the Maxwellian initial pulse into solitary waves. The numerical results show that the fully implicit finite difference method offers a high accuracy in the numerical solution of the EW equation.

References

[1] Ali A. H. A., Spectral method for solving the equal width equation based on Chebyshev polynomials, *Nonlinear Dyn.*, **51**, 59-70 (2008).

[2] Archilla B. G., A spectral method for the equal width equation, *J. Comput. Phys.*, **125**, 395-402 (1996).

[3] Arora R., Siddiqui Md. J., Singh V. P., Solutions of Inviscid Burgers' and Equal Width Wave Equations by RDTM, *Int. J. Appl. Phys. Math.*, **2**, 212-214 (2012).

[4] Dag I., Saka B., A cubic B-spline collocation method for the EW equation, *Math. Comput. Appl.*, **9**, 381-392 (2004).

[5] Dogan A., Application of Galerkin's method to equal width wave equation, *Appl. Math. Comput.*, **160**, 65-76 (2005).

[6] Esen A. , A numerical solution of the equal width wave equation by a lumped Galerkin method, *Appl. Math. Comput.*, **168**, 270-282 (2005).

[7] Esen A., Kutluay S., A linerized implicit finite-difference method for solving the equal width wave equation, *Int. J. Comput. Math.*, **83**, 319-330 (2006).

[8] Gardner L. R. T., Gardner G. A., Solitary waves of the equal width wave equation, *J. Comput. Phys.*, **101**, 218-223 (1992).

[9] Gardner L. R. T., Gardner G. A., Ayoub F. A., Amein N. K., Simulations of the EW undular bore, *Commun. Num. Meth. Eng.*, **13**, 583-592 (1997).

[10] Haq F., Shah I. A., Ahmad S., Septic B-Spline Collocation method for numerical solution of the Equal Width Wave (EW) equation, *Life Sci. J.*, **10**, 253-260 (2013).

[11] Khalifa A. K., Ali A. H., Raslan K. R., Numerical study for the equal width wave (EWE) equation, *Mem. Fac. Sci. Kochi Uni.*, **20**, 47-55 (1999).

[12] Morrison P. J., Meiss J. D., Carey J. R., Scattering of regularized-long-wave solitary waves, *Physica D*, **11**, 324-336 (1984).

[13] Ramos J. I., Explicit finite difference methods for the EW and RLW equations, *Appl. Math. Comput.*, **179**, 622-638 (2006).

[14] Raslan K. R., A computational method for the equal width equation, *Int. J. Comput. Math.*, **81**, 63-72 (2004).

[15] Raslan K. R., Collocation method using quartic B-spline for the equal width (EW) equation, *Appl. Math. Comput.*, **168**, 795-805 (2005).

[16] Saka B., A finite element method for equal width equation, *Appl. Math. and Comput.*, **175**, 730-747 (2006).

[17] Saka B., Dag I., Dereli Y., Korkmaz A., Three different methods for numerical solution of the EW equation, *Eng. Anal. Bound. Elem.*, **32**, 556-566 (2008).

[18] Zaki S. I., A least-squares finite element scheme for the EW equation, *Comput. Meth. Appl. Mech. Engrg.*, **189**, 587-594 (2000).

[19] Zaki S. I., Solitary waves induced by the boundary forced EW equation, *Comput. Meth. Appl. Mech. Engrg.*, **190**, 4881-4887 (2001).

Bilge İnan (bilgeinan@hotmail.com) –Department of Mathematics,Muallim Rifat Faculty of Education, Kilis 7 Aralik University, Kilis, Turkey

Ahmet Refik Bahadır –Department of Mathematics, Faculty of Arts and Science,İnönü University Malatyya, Turkey